EARTHQUAKE ENGINEERING AND STRUCTURAL DYNAMICS, VOL. 25, 15–30 (1996)

APPLICATION OF BOUNDARY ELEMENT ANALYSIS FOR MULTIPLE SEISMIC CRACKING IN CONCRETE GRAVITY DAMS

V. BATTA* AND O. A. PEKAU†

Department of Civil Engineering, Concordia University, Montreal, Canada H3G 1M8

SUMMARY

The previously developed two-dimensional boundary element procedure for analysing the propagation of a single discrete crack is extended to simultaneous multiple cracking in concrete gravity dams. A brief discussion of the generalized methodology is presented and the validity of the extended procedure is verified by performing a fracture analysis of the Fongman dam and comparing the predicted rupture process with the available experimental results. The fracture response of the Koyna dam is then studied extensively under the Koyna earthquake. Both single and multiple cracking models are employed to investigate the fracture process as well as final rupture in the dam. Similar final damage involving complete separation of the crest block of the dam is predicted, irrespective of whether single or multiple crack propagation models are employed. In relation to the phenomenon of hydrodynamic uplift pressure within propagating cracks, openings of the crack on the upstream face of the dam are examined in particular. The results indicate that this phenomenon is not expected to be significant during the crack development phase, and hence unlikely to affect the final rupture characteristics of dams undergoing strong earthquake excitation.

KEY WORDS: gravity dams; earthquakes; crack propagation; fracture mechanics; boundary elements

INTRODUCTION

Linear seismic response analyses, such as Reference 1, have demonstrated that concrete gravity dams subjected to strong ground shaking can develop tensile stresses in excess of the strength of concrete and crack. Non-linear procedures are therefore required to assess the seismic safety of concrete dams in earthquake-prone areas. These procedures generally involve either finite or boundary element mathematical models. Representation of the physical discontinuity introduced in the system by a crack is achieved by either separating the nodes belonging to crack flanks in the discrete crack approach[2,3] or by modifying the physical properties of the material in the zone of cracking when employing smeared crack modelling.[4,5] In either procedure, a suitable crack propagation criterion based on fracture mechanics principles needs to be adopted to monitor the progress of an unstable crack.

Employing the boundary element model of a dam monolith, propagation of a discrete crack in a concrete gravity dam (Koyna — India) was investigated by Pekau and Batta[6] and Pekau *et al.*,[7] with the latter also performing a laboratory rupture test of a model of the dam. A single initial crack was assumed in the dam and its propagation path, as well as the corresponding dam response, was studied using a linear elastic fracture mechanics criterion for crack extension. The positioning of the initial crack was based on a linear elastic analysis to predict the location and time of occurrence of the maximum principal tensile stress in the dam. These studies demonstrated the successful application of the boundary element technique and fracture mechanics principles in predicting the path followed by a single pre-assigned crack during strong earthquake ground shaking. Although these were the first attempts at employing the boundary element method for solving this complex non-linear problem, the procedures accounted for only a single crack in the dam.

In the present work, the procedure of Reference 6 is extended to the more general case where the occurrence and simultaneous propagation of multiple cracks can be simulated. The previously developed

*Adjunct assistant professor; also Structural Engineer, SNC-Lavalin Inc., Montreal
†Professor

CCC 0098–8847/96/010015–16

Received 28 December 1994
Revised 11 July 1995

boundary element formulation together with the linear elastic fracture mechanics crack extension criterion is kept largely unchanged, although a more elaborate numerical procedure is employed to monitor opening/closing, stability and propagation of multiple cracks. It should be noted that each new crack requires a subdivision of the dam domain along the crack profile; consequently, the presence of a large number of cracks makes the analysis increasingly complicated. Although many small cracks are usually present in a concrete dam (due to shrinkage, weathering, etc.) and others may initiate when the dam is subjected to an earthquake, during a strong seismic event only a few of these cracks actually propagate sufficiently deep into the body of the dam to endanger the safety of the structure. This has been observed both during the instances of seismic cracking in prototype dams and in available analytical[2-4] and experimental investigations.[8,9] Indeed, once a crack is formed it is likely to release the tensile stresses over a considerable depth above and below, thus preventing formation of other major cracks in nearby regions.

Since the details are available elsewhere,[10] the boundary element formulation is only briefly reviewed herein. The crack propagation criterion and the procedure for mathematically simulating opening and closing of simultaneous multiple cracks are also summarized. The extended numerical procedure is verified using the results of a model test conducted by Zhou and Lin.[9] This is followed by a detailed examination of the cracking process for the Koyna dam employing both single and multiple fracture models. Particular attention is focussed on the patterns of rupture predicted by these fracture models, as well as on the associated crack opening behaviours. The latter are of major interest in evaluating the possible development of hydrodynamic uplift pressure inside a propagating crack.

IMPLEMENTATION OF BOUNDARY ELEMENT METHOD

In the dynamic boundary element procedure employed herein, the equation governing scalar wave propagation in an elastic, isotropic and homogeneous medium is used to formulate the problem. The frequency-independent fundamental solution corresponding to an infinite domain is utilized as the weighting function to obtain the integral equation in the time domain. The domain integral equation so obtained is reduced to a boundary integral expression by employing Betti's reciprocal work theorem, together with a suitable transformation for the inertial domain integral. The resulting boundary-only integral expression represents the governing integral equation of the problem, which can be integrated numerically. This is achieved by dividing the domain boundary into discrete elements and employing standard isoparametric formulation to represent displacement and traction variation over the length of each element. The integral equation is thus converted to a matrix equation. Details of this procedure along with the various transformations are available in Reference 10.

In modelling a dam body containing discrete cracks, the boundary element technique requires that the crack surfaces, which obviously have identical spatial location, belong to two different dam domains. The crack flank nodes belong to the adjacent subdomains, whereas the common nodes along the interface ahead of the crack tip provide continuity of displacement and equilibrium of tractions between the two subdomains. The boundary of the system, as well as the interfaces between subdomains, is discretized and the global matrix equation is assembled.

Since the dam is a damped dynamic system subjected to external excitation, this matrix equation (or its incremental counterpart) takes the form

$$[m_{11}]\{\ddot{u}_r\} + [c_{11}]\{\dot{u}_r\} + [k_{11}]\{u_r\} = [m_o]\{\ddot{u}^o\} + \{Q_1\} \tag{1}$$

where $[m]$, $[c]$ and $[k]$ denote, respectively, the mass, damping and stiffness matrices of the system, with subscript '1' denoting the portion of the boundary on which no external excitation acts; $\{u_r\}$ represents the relative displacement vector with its time derivatives (velocity and acceleration) indicated by overhead dots; $\{\ddot{u}^o\}$ is the vector of external excitation; $[m_o]$ denotes the inertial matrix corresponding to those degrees-of-freedom on which the external excitation is applied; and $\{Q_1\}$ is a time-dependent nodal force vector obtained by suitably transforming the boundary traction vector. In problems involving significant static loads, such as the present gravity and hydrostatic loads on the concrete dam, the static load vector is added

to the right-hand side of equation (1). Although the Houbolt integration scheme is selected herein, any direct integration procedure can be pursued to obtain the time-domain solution of equation (1).

Modelling and monitoring of multiple cracks

Modelling of a single crack in a dam has been discussed previously and the same general principles apply when more cracks than one are present. For each crack, the surrounding domain is divided into subregions by extending a line from the crack tip to the opposite boundary. The direction of this line is completely arbitrary as it is only used to separate analytically the domains bordering the crack flanks. Each additional crack thus increases the number of subdomains by one. If any two cracks exist at nearly the same elevation but on opposite faces of the dam, the same arbitrary line could be employed as the dividing line, but in the present computer implementation separate lines are used to provide better control during rediscretization following crack propagation.

During the time step-by-step analysis, opening and closing of each crack are monitored continuously. The nodal displacement components normal to the crack surfaces are used for this purpose. At the instant when closure is predicted at a crack flank nodal pair, a stiff dimensionless spring is introduced at this location and the load vector is appropriately modified. If, on the other hand, opening is detected at a previously closed nodal pair, the corresponding spring is removed.

Since the present analysis of cracking in concrete gravity dams relies on linear elastic fracture mechanics, the corresponding analytical modelling of stress singularity at discrete crack tips is achieved by providing traction singular quarter-point elements. To simulate the induced mixed mode of cracking, both mode I and II stress intensity factors are computed employing the displacement correlation technique. Maximum tensile strain theory is employed to monitor crack stability, based on the dynamic fracture toughness K_{Id} as the only material parameter governing fracture. When a crack is detected to be unstable, the direction of crack propagation is computed and the boundary element mesh along the crack line is appropriately modified as discussed below.

Remeshing after crack extension

At each stage of crack extension remeshing is required so that the new crack tip, which is located in the computed direction at a pre-selected distance from the existing tip, can be integrated in the boundary element mesh. This requires that the nodes along the crack flanks, as well as on the interface ahead of the current crack tip, be suitably moved. Once the co-ordinates of the crack tip node are decided, those of the other nodes along the crack line are adjusted so that the resulting interface line has no abrupt change in direction. The mesh near the crack tip is redefined, keeping the length of the quarter-point element at the tip to within 10–15 per cent of the current crack length in order to ensure accurate computation of stress intensity factors. The remaining elements on the crack surfaces and the interface are relocated accordingly, maintaining a fairly fine mesh in the vicinity of the crack tip. As the crack grows, new nodes are also required to be added along the crack line to preserve desirable mesh density. Note that the arbitrary line shifts continuously, but always extends from the current crack tip position to a node on the opposite face of the dam. The rest of the boundary element mesh is, however, not disturbed.

If during the analysis multiple cracks lie close to each other, it is possible that one of the crack tips advances towards the interface line corresponding to an adjacent crack. In such a case, the affected subdomain boundary needs to be relocated to accommodate the extending crack. The problem can be more easily circumvented by choosing judiciously the initial orientations of the interface boundaries so that they are less likely to interfere with crack development.

Choice of analytical factors influencing fracture analysis

As noted in Reference 6, in the foregoing formulation for discrete crack propagation two other analytical factors should be considered, namely the inclusion of interior domain collocation and the magnitude of incremental crack extension. It was also noted that boundary-only discretization is adequate for seismic

fracture analysis of concrete gravity dams, since the dynamic response is primarily contained in the first 4 or 5 vibration modes. No interior nodes are therefore defined in the analyses presented in the following sections.

On the other hand, the choice of a suitable magnitude for crack extensions is important because it affects directly the computational efficiency and possibly also the predicted crack path itself. Based on the results of the parametric investigation reported in Reference 6, a piecewise extension of 10 per cent of the instantaneous crack length, but limited to a maximum increment of 1·0 m, is employed in the following crack propagation analyses of the prototype Koyna dam. For the model dam application, the corresponding increment is 2 per cent with a maximum permitted extension of 25 mm.

Applications

In the following, the seismic cracking responses of the Fongman and the Koyna concrete gravity dams are presented. The Fongman dam is employed in order to confirm the validity of the present numerical procedure to simulate multiple crack propagation. On the other hand, the Koyna dam has been analysed extensively in previous investigations, and studied herein also since it provides the only example of a gravity-type concrete dam where significant cracking occurred during a seismic event soon after construction.

MULTIPLE CRACKING OF FONGMAN DAM

Fongman dam, situated in northeast China, is a 77·5 m high concrete gravity dam which has previously been used as an example problem for studying earthquake-induced cracking by Zhou and Lin.[9] In their investigation two initial horizontal cracks were introduced on the upstream face of the dam. Seismic stability as well as unstable propagation of these cracks under ground shaking were studied numerically. A laboratory model of this dam, scaled at a dimensional ratio of 1:40 and made of gypsum, was also tested on a shaking table.

The present analysis of this laboratory model of the dam is based on the boundary element discretization depicted in Figure 1(a). The lower crack, 775 mm from the base, is designated as C1 while the upper crack, at 490 mm from the crest, is labelled as C2. Initial lengths of these cracks are, respectively, 275 and 250 mm. The

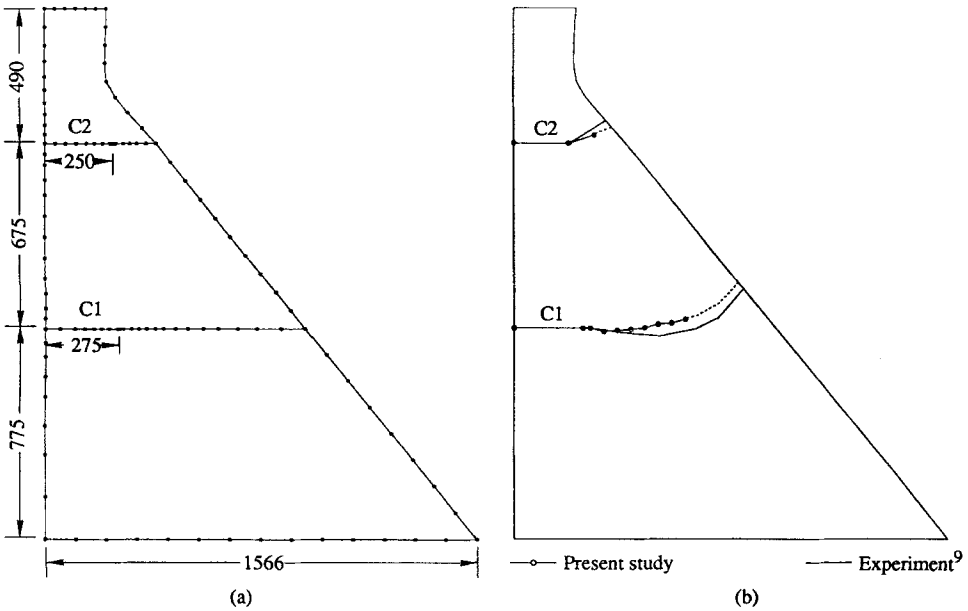

Figure 1. Fongman dam model with initial cracks: (a) boundary element discretization; (b) final cracking profiles

model is considered fixed at the base and with no reservoir in order to match the boundary conditions of the experiment.

The boundary element mesh consists of 129 nodes and 70 quadratic boundary elements. Three traction singular quarter-point elements are employed at each crack tip, two on the crack flanks and one ahead of the tip. The following material properties of the gypsum consistent with reported values are used in the analysis: dynamic modulus of elasticity $E_d = 1650$ MPa; Poisson's ratio $\nu = 0{\cdot}2$; mass density $\gamma = 665$ kg/m^3; and damping equal to 1·5 per cent of critical for the first mode.

The dynamic fracture toughness of the gypsum is not mentioned in Reference 9 and is computed from similitude relations to be 25 kPa m$^{1/2}$, corresponding to fracture toughness of 1·5 MPa m$^{1/2}$ for the dam concrete. The computed modal frequencies of the model dam are compared against those obtained from the laboratory test. For the first two modes the computed natural frequencies are 59·6 and 125·0 Hz, in good agreement (average difference 6·7 per cent) with the corresponding test frequencies of 62·05 and 138·05 Hz. As in the test, harmonic excitation at the natural frequency of the fundamental mode is assumed at the base.

The predicted final crack profiles are presented in Figure 1(b) and compared with experimental results. Good agreement is evident. In the analysis, lower crack C1 propagates first, but stabilizes after extending in two stages by a total of only 94 mm. Immediately thereafter, upper crack C2 becomes unstable and propagates quickly to approach the downstream face. Once the tip of this crack is sufficiently close to the downstream face, further propagation cannot be modelled and complete separation along crack C2 is predicted. Such complete rupture in the upper part of the dam is not likely to influence significantly the subsequent response of the lower portion, as long as the separated crest block remains in place. Since this was indeed the case during the laboratory test, the continuation of the analysis with almost complete separation along crack C2 can be expected to predict adequately the response of lower crack C1. With crack C2 artificially arrested near the downstream face, in the continued analysis crack C1 resumes propagation also to penetrate through the dam. As in the case for C2, once the tip of crack C1 reaches close to the downstream face further remeshing is not possible and rupture is assumed. In the laboratory test, the two initial cracks also propagated to penetrate completely through the dam, after which the separated upper portions continued to rock after rupture. The computed times of crack extensions indicate that both cracks grow very quickly to reach the opposite face, a feature also noticed in the model test.

SINGLE AND MULTIPLE CRACKING OF KOYNA DAM

Koyna dam is a 103 m high concrete gravity dam in India which was constructed in 1963 and subjected to magnitude 6·5 earthquake on 11 December 1967. Peak acceleration of 0·49 g in the stream direction, 0·63 g in the cross-stream direction and 0·34 g vertical were recorded in a monolith near one of the abutments. Strong ground shaking lasted approximately 4 sec. Significant horizontal cracking was noticed in a number of the non-overflow monoliths on the upstream, the downstream or on both faces. Leakage was observed in some of these monoliths from approximately horizontal cracks near the elevation of slope change on the downstream face, thus implying complete penetration from one face to the other.

The cross-section of the tallest non-overflow monolith of this dam is shown in Figure 2(a). The dam has this non-typical cross-section due to a change made during construction when it was decided to build the dam to its full height in one stage rather than the planned two phases. In the analysis, the following material characteristics are used for the concrete: modulus of elasticity $E = 31$ GPa; Poisson's ratio $\nu = 0{\cdot}2$; and mass density $\gamma = 2640$ kg/m^3. The concrete compressive and tensile strengths are assumed to be 30 and 3 MPa, respectively. In the absence of any test data for the Koyna concrete, K_{Id} is assumed to be 2·0 MPa m$^{1/2}$, which is slightly higher than the commonly used static fracture toughness of 1·5 MPa m$^{1/2}$. The influence of further increasing the magnitude of this parameter to 5·5 and 9·0 MPa m$^{1/2}$ is also investigated. This range of values has been employed because the fracture toughness of concrete depends not only on the composition of the concrete but also on the size of the specimen tested,[11] as well as on the loading rate in a dynamic environment.[12] Increasing magnitudes of the latter two parameters increase the toughness. Moreover, it has been demonstrated previously[6] that, for higher magnitude of the fracture toughness and a single propagating

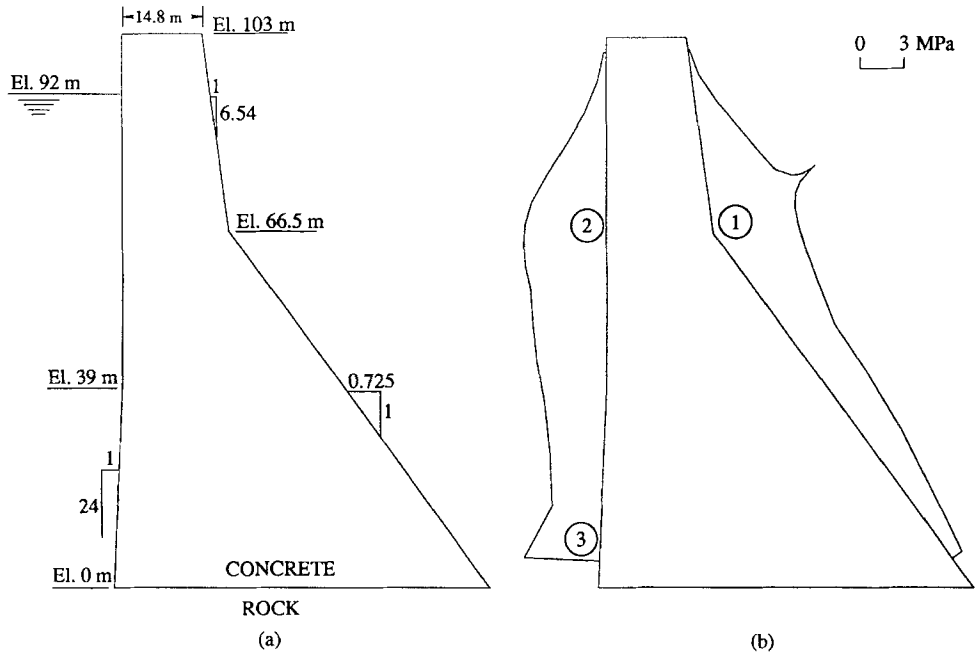

Figure 2. Koyna dam: (a) tallest non-overflow monolith; (b) envelope of principal tensile stresses for seismic analysis without cracks

crack, sufficiently high tensile stresses occur at a number of points in the dam to cause the initiation of multiple cracks.

Since the foundation medium at the Koyna dam site comprises competent rock, with an estimated Young's modulus of 70 GPa which is more than twice that of the concrete, the dam can be considered fixed at the base, thus neglecting interaction with the foundation rock. A full reservoir is assumed with the water level at 11 m below the crest, which corresponds to the level when the earthquake occurred. The hydrodynamic effect of the reservior water is modelled approximately by Westergaard added mass with the water considered incompressible. Damping equal to 5 per cent is assumed for the first two modes of vibration and an integration time step of 0·005 sec is employed.

Water pressure effects in the cracks are not included in the analysis, since no model for hydrodynamic interaction in cracks propagating under seismic action exists to the authors' knowledge and opinions also differ concerning the importance of this phenomenon. The recent study by Tinawi and Guizani[13] comprises the first attempt at examining the problem analytically. Although it does demonstrate the significance of hydrodynamic pressure inside cracks, the procedure is applicable only for short pre-existing open cracks* and does not address the question of pressure development within a propagating crack. In engineering practice, the commonly used agency guidelines include those of the U.S. Bureau of Reclamation (USBR)[14] and U.S. Federal Energy Regulatory Commission (FERC).[15] The FERC guidelines assume that the initial uplift pressure in a crack remains unchanged during an earthquake, whereas the Bureau guidelines assume that the internal water pressure is relieved completely when a crack opens during an earthquake. The justification given for these assumptions is that a crack will open and close cyclically in quick succession during strong ground shaking, thus inhibiting the water pressure to react. The opening/closing behaviour of the cracks is therefore monitored closely in the results presented herein in an attempt to obtain appropriate data associated with this phenomenon.

*Under non-seismic loadings including internal pore-water uplift over the dam cross-section, the initial upstream cracks considered in this study were found to remain closed and stable, with stresses all compressive.

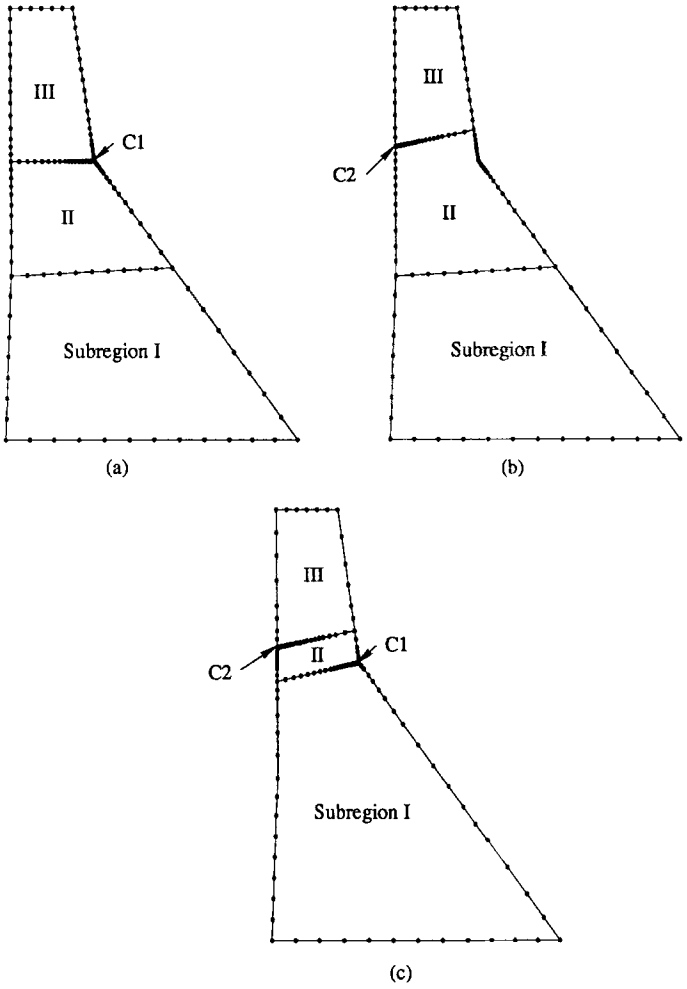

Figure 3. Boundary element discretizations of Koyna dam for different fracture models: (a) single downstream crack C1; (b) single upstream crack C2; (c) multiple cracking

Potential cracking models

In order to predict the locations of potential cracking, stress analysis of the intact dam subjected to 6 sec of vertical and horizontal accelerations of the recorded Koyna earthquake as well as the static loads (concrete dead weight plus reservior hydrostatic pressure) is first performed. Envelopes of the resulting principal tensile stresses on the faces of the dam are presented in Figure 2(b), where it is seen that the tensile stresses exceed the tensile strength of concrete near elevation 66·5 m on both the downstream and the upstream faces (zones 1 and 2, respectively). On the downstream face, due to the change in slope at this elevation, the stress singularity results in a computed maximum tensile stress almost three times the tensile strength of concrete. Another zone of high tensile stress is obtained on the upstream face near the base (zone 3). However, since the observed cracking in the Koyna dam is limited to zones 1 and 2 only, in the present study cracking of the dam is investigated in these regions. Fracture in zone 3 was also considered but an initial crack modelled at this location did not propagate during seismic analysis.

Based on the above, three different sets of small cracks are pre-assigned on the faces of the dam and the fracture response of the dam is investigated for each of these three models of cracking. In the first two, a single 1 m long initial crack is introduced separately on the downstream and the upstream faces of the dam, cracks

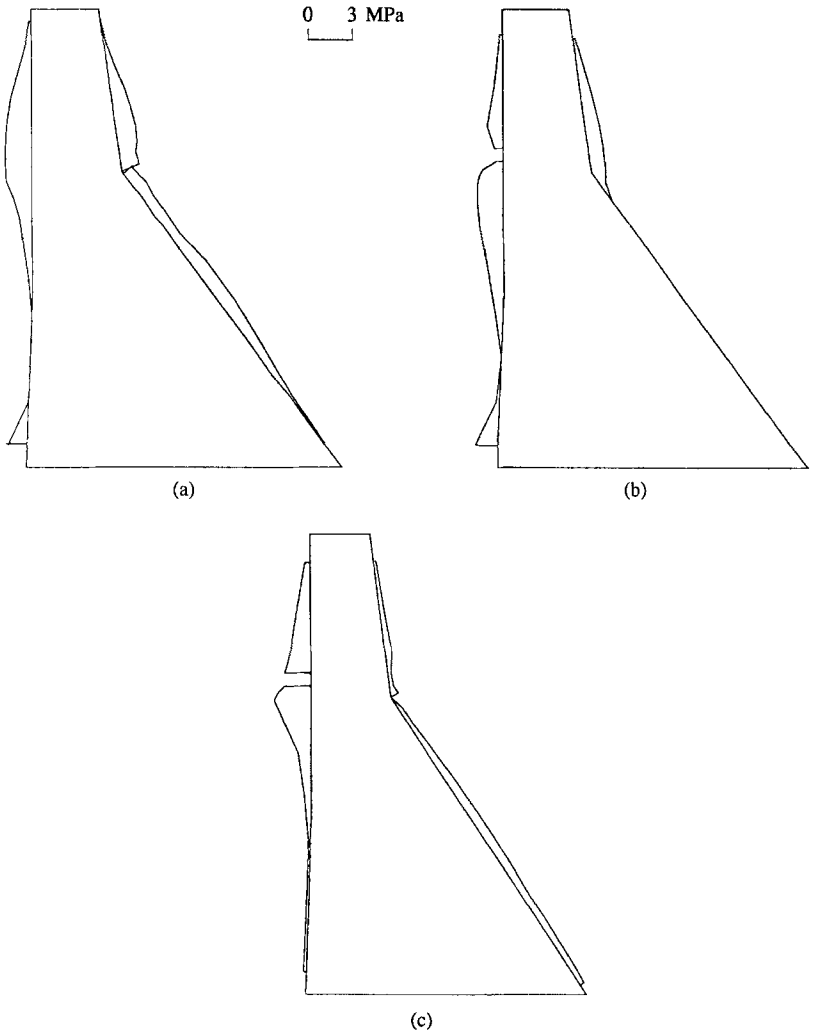

Figure 4. Envelopes of principal tensile stresses for different fracture models: (a) single downstream crack C1; (b) single upstream crack C2; (c) multiple cracking

C1 and C2 at elevations 66·5 and 70·0 m, respectively, whereas in the third case a multiple cracking model is assumed with cracks C1 and C2 originating simultaneously on both faces of the dam. The corresponding boundary element discretizations for these cracking models are depicted in Figure 3. As shown, the initial crack(s) and the arbitrary line(s) emanating from the crack tip(s) are used to divide the dam domain into appropriate subregions. For the fracture models involving single cracks, an additional subdomain is defined to provide more degrees-of-freedom and to reduce the domain integration area below the crack. In the multiple cracking model, the presence of additional nodes along the second crack line supplies the additional degrees-of-freedon and further subzoning is therefore not adopted.

Envelopes of the principal tensile stresses on the faces of the dam are presented in Figure 4 for the three cracking models. For the models with a single crack propagating from either the downstream or the upstream face, Figures 4(a) and 4(b) show that the tensile stresses on both faces of the dam are reduced to levels below the strength of concrete. Thus, it appears that, if the initial cracking originates on either face, other cracking will not develop before the initial crack has broken through to the opposite face. Similar behaviour is observed in Figure 4(c) for cracks C1 and C2 propagating from both faces. Unlike the preceding

two fracture models, however, this analysis was able to be continued for a substantially longer period of time prior to rupture, allowing the dam to be subjected to the more intense portion of the Koyna earthquake. In spite of this increase in ground shaking, the stress release caused by cracking is seen still to reduce the maximum tensile stress to below the strength of the concrete. Simultaneous other cracking is therefore not predicted to occur in the dam for this fracture model also.

It is therefore evident that the model for the actual cracking of the dam is most likely to be associated only with zone 1. Not only does the change in slope provide a singular point for first crack formation, this crack also breaks through the dam before cracking can be initiated at other locations. However, because initial cracks are not solely stress-induced but may also arise due to a variety of other causes including shrinkage, temperature effects, etc., the additional two fracture models are included in the following examination of the fracture process of the Koyna dam. Moreover, for dams of other geometries involving more typical cross-sections, all the above three cracking models become possible candidates for the critical fracture process. Even for the Koyna dam, a previous finite element analysis based on the discrete crack approach[3] as herein, as well as laboratory rupture testing,[8] have indicated fracture behaviour corresponding to the current single C1 cracking model, whereas other studies which employed either smeared crack modelling[4] or a quite high concrete fracture toughness[2] have predicted final fracture patterns similar to the present multiple cracking model.

Comparison of fracture processes for single and multiple cracking models

Results for seismic crack propagation with initial cracks C1 and C2 considered separately are presented in Figures 5 and 6, respectively, whereas Figure 7 depicts the results for the multiple fracture model wherein C1 and C2 are treated simultaneously. As shown in Figures 5(a) and 6(a), the final cracking profiles for the single fracture models are more or less similar, with the initial crack breaking through to the opposite face of the dam to cause complete rupture. Analogous final behaviour is predicted by the multiple fracture analysis, in which cracks C1 and C2 merge within the body of the dam and also result in full separation of the crest block as seen in Figure 7(a). However, the final rupture pattern for the multiple cracking model differs markedly from the profiles of the single fracture models.

In the absence of other cracking, crack C1 of Figure 5(a) propagates smoothly and emerges close to El. 64 m on the upstream face. Similarly, when only upstream initial crack C2 is considered [Figure 6(a)], the crack travels toward the zone of high compression occurring at the point of slope change on the downstream face. For the multiple cracking model, however, it is apparent from Figure 7(a) that the presence of crack C2 alters the profile of downstream crack C1 during its final stages of propagation. In this fracture model crack C1 completes its propagation while upstream crack C2 is still short; consequently, the influence of C2 on crack C1 is only evident toward the end of the propagation of the latter. On the other hand, the final trajectories of crack C2 are noticeably different in Figures 7(a) and 6(a). With crack C1 already developed in Figure 7(a) for the multiple cracking model, a change in the orientation of the stress field in front of the crack tip causes C2 to bend downwards. This change in stress field orientation is due to the increase in shear stress which occurs in the intact concrete ahead of the crack tip when the crest deflects in the downstream direction. In this process, the tip of this crack approaches sufficiently close to crack C1 so that further propagation analysis would cause the subdomain boundaries emanating from the two crack tips to intersect. It is therefore assumed that the upstream crack merges into the downstream crack at this time, resulting in complete rupture along the dashed line in Figure 7(a).

As is to be expected, the above more complicated cracking pattern associated with the multiple cracking model increases the computational effort. In terms of the remeshing, a total of 30 rediscretizations is required to trace the propagation of cracks C1 and C2, whereas 20 rediscretizations suffice for the smoother profiles of single crack models 1 and 2.

It is noteworthy that crack propagation is not necessarily in phase with the displacement of the crest of the dam. For example, it is found that the crest displacement associated with Figure 6 attains its peak value of 15·15 mm at 2·26 sec, whereas instability of the crack occurs only two time steps later, at 2·27 sec when the crest has already begun to move toward the upstream. Flexibility of the structure is the explanation for this

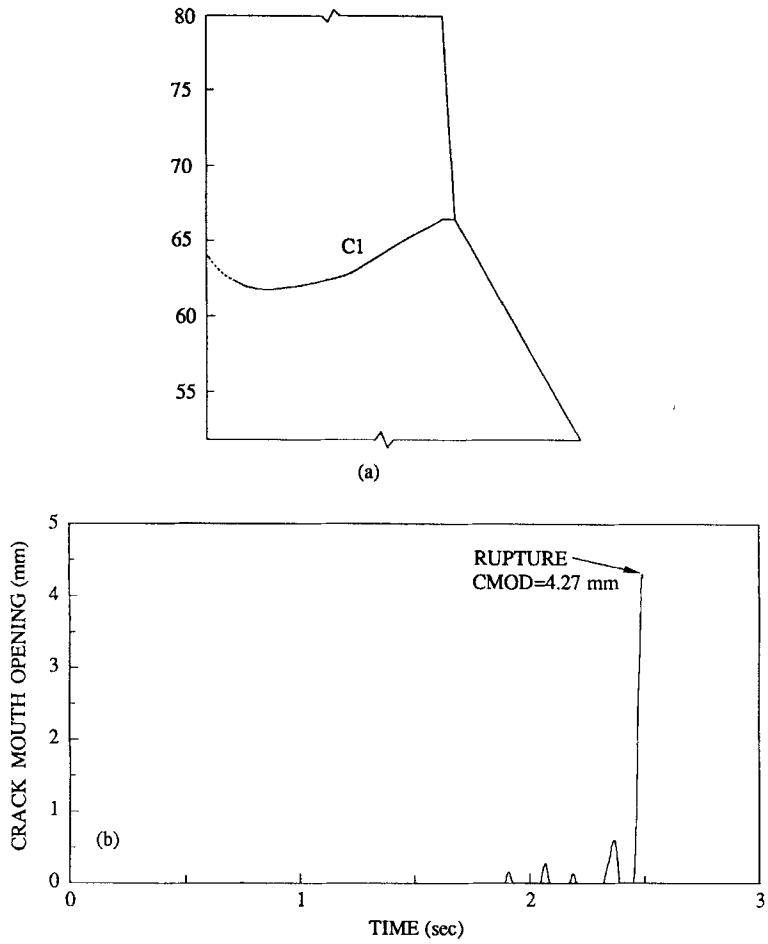

Figure 5. Fracture process for single downstream crack C1: (a) final cracking profile; (b) time history of crack mouth opening

phase difference, as a result of which the relative displacements along crack flanks are not directly related to the crest displacement.

In order to examine the possible development of hydrodynamic uplift pressure in cracks, the opening responses of the crack mouth are examined in Figures 5(b), 6(b) and 7(b) for the three fracture models. Although only the opening/closing behaviour of crack C2 on the water retaining face of the dam is relevant for this phenomenon, results are also presented for downstream crack C1 as an indication of seismic damage on this face of the dam. From the time histories of the crack mouth opening displacements of Figures 5(b) and 6(b) for the single fracture models, it is evident that the cracks remain more or less closed for almost the entire time. Noting that the critical openings to initiate propagation of C1 and C2 are 0·760 and 0·304 mm, respectively, it is also evident that the first major crack mouth opening coincides with rupture. For propagation of single crack C1 the crack mouth opening at rupture is 4·27 mm, with a corresponding magnitude of 3·9 mm for crack C2.

In comparison, Figure 7(b) shows that the crack opening behaviour predicted by the multiple fracture model is very different. Downstream crack C1 is first to propagate (at mouth opening of 0·348 mm for this model) and experiences dramatic increases in the magnitude of opening compared to the corresponding single crack model. While the two stages of propagation of this crack are associated with relatively large crack mouth openings at approximately 2·5 and 3·0 sec, these or even larger openings do not necessarily induce instability at the crack tip, due also to the forementioned flexibility of crack flanks with increasing

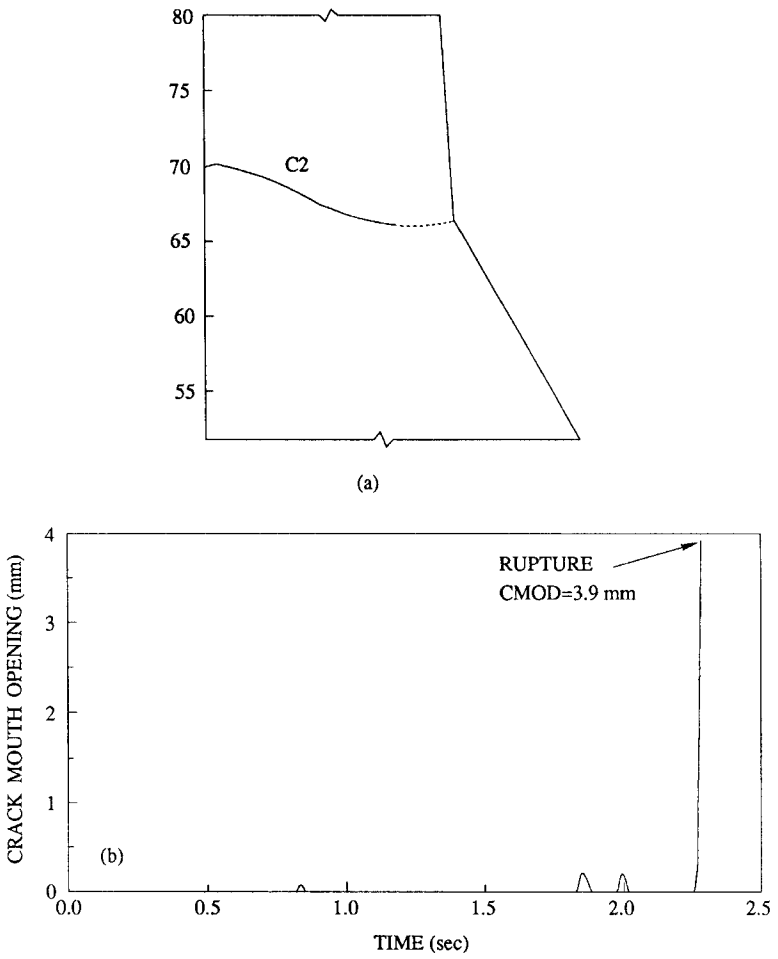

Figure 6. Fracture process for single upstream crack C2; (a) final cracking profile; (b) time history of crack mouth opening

crack length. During the opening at 3·0 sec, the crack extends in length until the magnitude of the opening is 5·5 mm, after which the crack does not propagate, although the crack mouth opening continues to increase to almost double this magnitude. The effect is even more strongly reflected during the subsequent opening of this crack at 4·0 sec, when the crack mouth opens by 43·7 mm but with crack instability not incurred.

Figure 7(b) also shows that crack C2 of this fracture model experiences similar dramatic, but opposite, change in mouth opening behaviour compared to the corresponding single cracking results of Figure 6(b). Unlike the above behaviour of crack C1, the openings of upstream crack C2 appear insignificant, with maximum predicted opening of 1·8 mm just prior to rupture and an even smaller magnitude of the opening of 1·1 mm at the time of final rupture.

Behaviour with higher concrete fracture toughness

As mentioned before, the cracking behaviour of the dam is also investigated for two higher values of the concrete fracture toughness, namely 5·5 and 9·0 MPa $m^{1/2}$. Since multiple cracking has been predicted previously[6] for higher magnitudes of concrete fracture toughness, the analysis is performed only for the multiple fracture model. As for the case with K_{Id} = 2·0 MPa $m^{1/2}$, an initial crack in zone 3 on the upstream face near the base of the dam was also considered but found not to propagate.

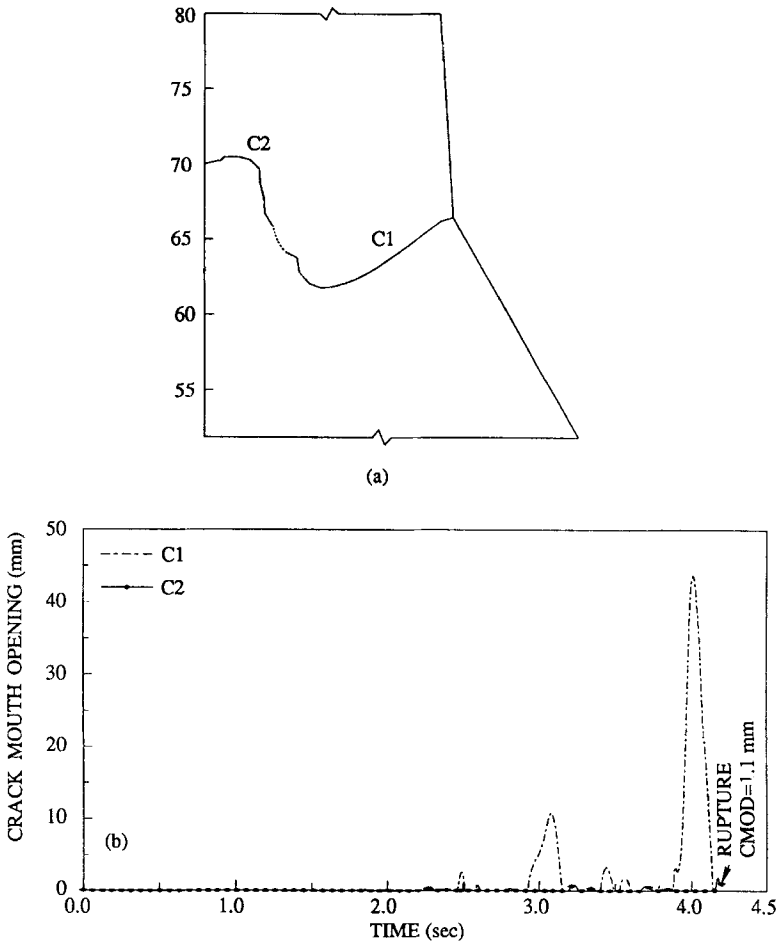

Figure 7. Fracture process for multiple cracking model: (a) final cracking profile; (b) time histories of crack mouth openings

The final crack trajectories for these two toughness values are presented in Figure 8. It is evident that substantially different cracking patterns are obtained for $K_{Id} = 5{\cdot}5$ and $9{\cdot}0\,\text{MPa}\,\text{m}^{1/2}$. For $K_{Id} = 5{\cdot}5\,\text{MPa}\,\text{m}^{1/2}$ the two cracks propagate into the dam and merge with each other, resulting in complete separation of the crest block. On the other hand, for $K_{Id} = 9{\cdot}0\,\text{MPa}\,\text{m}^{1/2}$ also downstream crack C1 propagates deep into (but not through) the dam, whereas the upstream crack is arrested after only about a meter of propagation. Comparison of Figures 8(a) and 7(a) indicates that the final rupture patterns are very similar for $K_{Id} = 2{\cdot}0$ and $5{\cdot}5\,\text{MPa}\,\text{m}^{1/2}$, although the details of the associated crack propagation processes (not discussed herein) differ considerably.

In the absence of any significant upstream cracking for $K_{Id} = 9{\cdot}0\,\text{MPa}\,\text{m}^{1/2}$, the principal tensile stress envelope for this case is examined in Figure 9. The delayed propagation of the downstream crack, due to the high fracture toughness combined with the short final length of the upstream crack, results in keeping the tensile stresses high throughout the dam faces. Comparing this envelope with that of the uncracked dam [Figure 2(b)] reveals that the stresses are almost identical over most of the dam. This is because the high values in the present case are reached before the downstream crack even begins to propagate. Thus, it appears that higher magnitude of concrete fracture toughness indeed results in distributing the surface cracking in the dam as predicted previously, but these cracks do not necessarily propagate if the concrete toughness is sufficiently high.

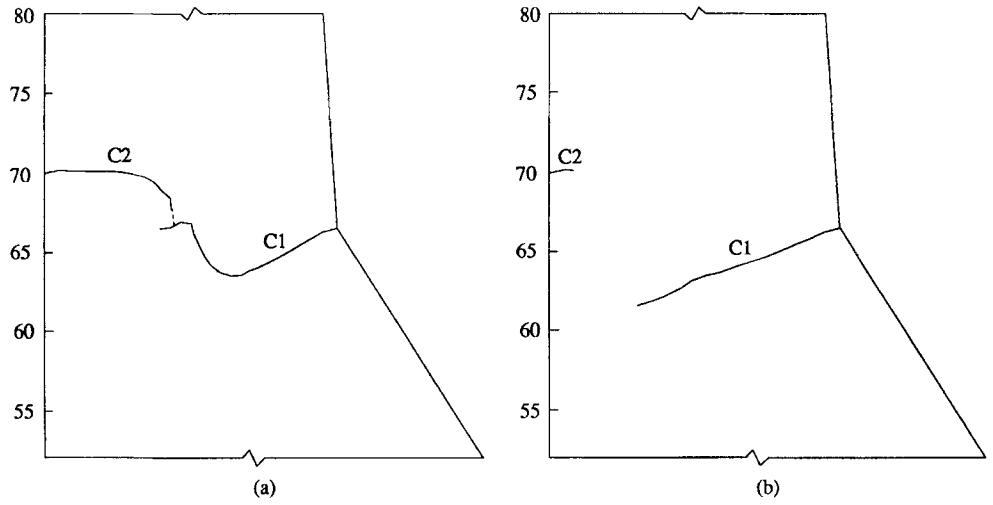

Figure 8. Final cracking profiles for multiple fracture model and higher magnitudes of dynamic fracture toughness: (a) $K_{Id} = 5{\cdot}5$ MPa m$^{1/2}$; (b) $K_{Id} = 9{\cdot}0$ MPa m$^{1/2}$

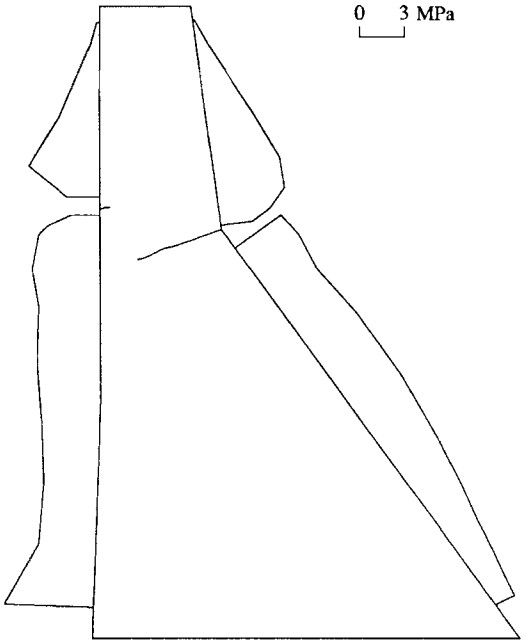

Figure 9. Envelope of principal tensile stresses for multiple cracking model and $K_{Id} = 9{\cdot}0$ MPa m$^{1/2}$

Post-rupture behaviour based on multiple cracking model

Although the maximum opening of upstream crack C2, for which hydrodynamic pressure is under question, has been observed to be small during the growth phase of the crack, the rocking of the separated crest block may still lead to the development of significant uplift pressure during the post-rupture phase. In order to estimate both the magnitudes and durations of these openings, the time history analyses for the multiple cracking model corresponding to the two lower values of the concrete fracture toughness are continued even though the cracks are predicted to have merged. For $K_{Id} = 9{\cdot}0$ MPa m$^{1/2}$, where the crest

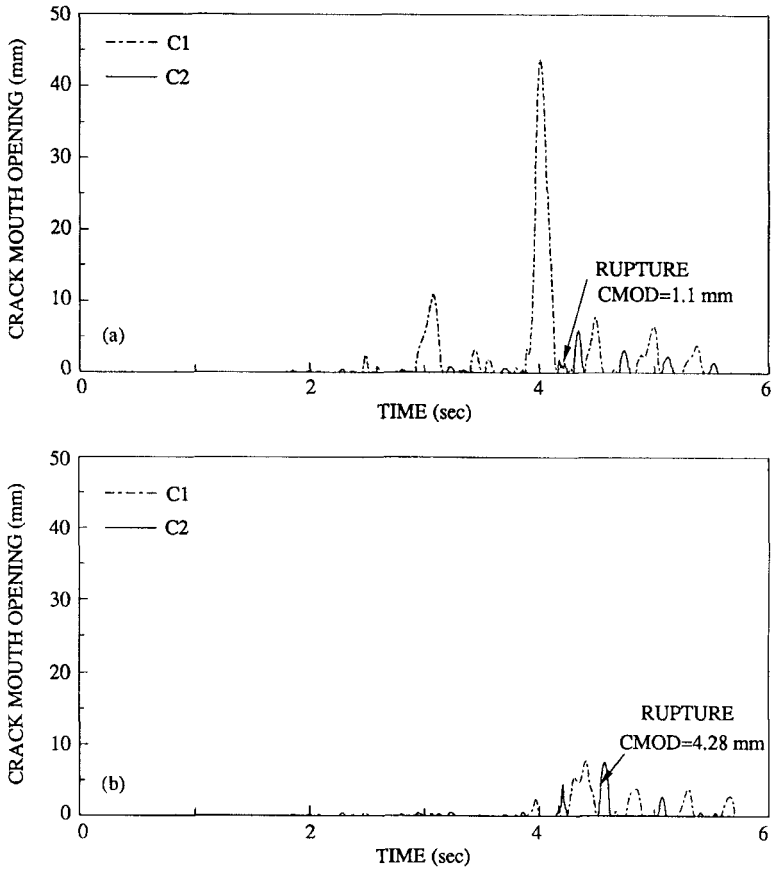

Figure 10. Post-rupture behaviour for multiple cracking model: (a) $K_{Id} = 2{\cdot}0\ \text{MPa m}^{1/2}$; (b) $K_{Id} = 5{\cdot}5\ \text{MPa m}^{1/2}$

block remains attached to the dam, it is found that the upstream crack openings remain very small for the entire duration of the applied excitation.

In order to undertake this approximate post-rupture analysis, the boundary element discretization is not updated for the last stage of extension of upstream crack C2 and the small portion of concrete between the two crack tips is left intact. The results can be viewed as realistic for the post-cracking behaviour based on the consideration that the intact portion is small and near the neutral axis of the cross-section. The imposed discontinuity in an otherwise through crack will therefore not significantly constrain the opening of the crack during further earthquake excitation. Furthermore, it can easily be demonstrated that sliding of the ruptured crest block is not likely to occur under the less intense base acceleration during the remaining time history of ground excitation.

The resulting complete time histories of crack mouth opening for $K_{Id} = 2{\cdot}0$ and $5{\cdot}5\ \text{MPa m}^{1/2}$ are plotted in Figure 10. For $K_{Id} = 2{\cdot}0\ \text{MPa m}^{1/2}$, Figure 10(a) shows that the magnitudes of opening of upstream crack C2 are much more pronounced during the post-rupture response compared to the pre-rupture phase. The crack remains more or less closed during almost the entire time prior to predicted rupture. As noted previously, the maximum opening of this crack is 1·8 mm immediately preceding rupture, with a corresponding magnitude at rupture of 1·1 mm. Compared to these, the post-rupture maximum opening increases to 5·9 mm. The associated duration is, however, only 0·1 sec and the durations of the other less prominent openings are also short. For downstream crack C1, on the other hand, the post-rupture openings are found to be reduced to a maximum of 7·7 mm from the aforementioned 43·7 mm immediately prior to rupture. Similar magnitudes of opening at the base of the ruptured crest block have also been reported by Saini and Krishna,[16] who

Table I. Crack mouth opening data for C2

K_{Id} (MPa m$^{1/2}$)	Mouth opening data	Pre-rupture		Rupture		Post-rupture
		Single fracture model	Multiple fracture model	Single fracture model	Multiple fracture model	Multiple fracture model
2·0	Magnitude (mm)	0·21	0·80	3·90	1·80	5·90
	Duration (sec)	0·05	0·07	0·03	0·06	0·09
	Time (sec)	1·85	3·23	2·28	4·21	4·34

performed a simplified seismic stability analysis of the separated top profile of the dam. When subjected only to the streamwise component of the Koyna earthquake, they obtained a maximum opening of approximately 33 mm at the face of the rocking block, in reasonable agreement with the 43·7 mm predicted herein since crack C1 is nearly fully developed across the dam cross-section at the time of this opening.

Post-rupture crack mouth behaviour generally similar to the above is predicted for $K_{Id} = 5{\cdot}5$ MPa m$^{1/2}$ in Figure 10(b), although the differences between the pre- and post-rupture magnitudes are not as dramatic as for $K_{Id} = 2{\cdot}0$ MPa m$^{1/2}$. The maximum opening of upstream crack C2 is 7·6 mm in the post-rupture phase compared to 4·31 mm shortly before rupture. The corresponding magnitudes for crack C1 are 3·8 and 7·8 mm. The time during which the critical crack C2 remains open is small for this fracture toughness also, generally less than 0·1 sec.

Summary of observations concerning development of hydrodynamic pressure in crack C2

Since the development of dynamic uplift pressure in upstream cracks is directly related to their opening/closing behaviour, the mouth opening data for crack C2 on the water retaining face of the dam are summarized in Table I for the practical case of $K_{Id} = 2{\cdot}0$ MPa m$^{1/2}$. The data are compiled for the three phases of the fracture response of the dam: namely, prior to rupture, at the time of predicted rupture and during the post-rupture response. It is evident that the opening response of the crack in the pre-rupture phase is more or less independent of the fracture model used and both the maximum magnitude and corresponding duration are very small. The largest opening is 0·8 mm with a duration of 0·07 sec. Thus, it appears that the opening of the crack is expected to not be sufficient to allow the hydrodynamic pressure to build up prior to the time of rupture and hence unlikely to influence the pre-rupture response. Furthermore, as demonstrated by Tinawi and Guizai,[13] for crack openings smaller than 1·0 mm the effect of viscosity of the water inside a crack becomes important. For the above small pre-rupture openings, the resulting additional damping is therefore likely to reduce the opening response of the crack further.

In comparison to the above pre-rupture observations, considerably larger magnitudes of opening are predicted at rupture itself, as well as in the analysis following separation of the crest block. As indicated in Table I, the maximum opening is 3·9 mm at the time when the crack breaks through the dam and 5·9 mm during the response following rupture. Although the associated durations of these openings are still small (also less than 0·1 sec), it appears that the opening magnitudes of this order could result in the dynamic uplift pressure penetrating the crack and affecting the post-fracture response of the dam.

It is noteworthy that a comparable magnitude of the opening of the upstream crack mouth has been reported by Bhattacharjee and Leger.[4] In their study which included also the post-rupture response, the crack opens by a maximum of 6·8 mm on the upstream face of the dam, although the cracking develops at a lower elevation and a slightly smaller magnitude of concrete fracture toughness $K_{Id} = 1{\cdot}5$ MPa m$^{1/2}$ was employed. The corresponding magnitude predicted in the present investigation is 5·9 mm in Table I.

CONCLUSIONS

The performance of the boundary element procedure for the analysis of multiple cracking in concrete gravity dams has been demonstrated in this work. For the Koyna dam, the critical cracking is found to be associated

with fracture originating at the point of downstream slope change and penetrating the dam almost instantaneously. Other possible patterns of initial cracks, including cracks propagating from both faces of the dam, also result in complete rupture although the fracture process itself is considerably different for the multiple cracking model when compared with those for single fracture. Increasing the concrete fracture toughness from 2·0 to 5·5 MPa $m^{1/2}$ does not appear to affect the predicted final cracking in the dam, but the opening/closing response of cracks is altered considerably due to the delay in the initiation of crack propagation for the latter. Furthermore, for higher magnitudes of toughness cracking in the dam becomes distributed but with most of the cracks confined to the surface. Concerning the opening of the upstream crack and the possible development of hydrodynamic pressure, it is found that the upstream crack exhibits fairly small openings during the pre-rupture response, probably sufficient to inhibit the build-up of significant dynamic uplift pressure. However, at rupture and during the post-rupture response, considerably larger magnitudes of opening are predicted which could be sufficient for the development of hydrodynamic pressure. The time intervals during which the upstream crack remains open are however small, usually less than one-tenth of a second. Further research, both analytical and experimental, is therefore required to investigate the role of this phenomenon during these stages of the seismic response.

ACKNOWLEDGEMENTS

This research was supported by Grant No. A8258 from the Natural Sciences and Engineering Research Council of Canada. The advice of Professor Zhang Chuhan of Tsinghua University, Beijing, during various stages of this work is also gratefully acknowledged.

REFERENCES

1. A. K. Chopra and P. Chakrabarti, 'The Koyna earthquake and damage to Koyna dam', *Bull. seism. soc. Am.* **63**, 381–397 (1973).
2. M. L. Ayari and V. E. Saouma, 'A fracture mechanics based seismic analysis of concrete gravity dams using discrete cracks', *Eng. fract. mech.* **35**, 587–598 (1990).
3. D. Wepf, P. Skrikerud and H. Bachmann, 'Influence of cracking on the seismic response of concrete gravity dams', *Proc. 8th world conf. on earthquake engineering*, San Francisco, 1984, pp. 95–102.
4. S. S. Bhattacharjee and P. Leger, 'Seismic cracking and energy dissipation in concrete gravity dams', *Earthquake eng. struct. dyn.* **22**, 991–1007 (1993).
5. L. M. Vargas-Loli and G. L. Fenves, 'Effects of concrete cracking on the earthquake response of gravity dams', *Earthquake eng. struct. dyn.* **18**, 575–592 (1989).
6. O. A. Pekau and V. Batta, 'Seismic cracking behavior of concrete gravity dams', *Dam eng.* **5**, 5–29 (1994).
7. O. A. Pekau, Feng Lingmin and Zhang Chuhan, 'Seismic cracking of Koyna dam: case study', *Earthquake eng. struct. dyn.* **24**, 15–33 (1995).
8. A. Niwa and R. W. Clough, 'Shaking table research on concrete dam models', *Report No. UCB/EERC 80/05*, Earthquake Engineering Research Center, University of California, Berkeley, September 1980.
9. Jing Zhou and Gao Lin, 'Seismic fracture analysis and model testing of concrete gravity dams', *Dam eng.* **3**, 35–47 (1992).
10. O. A. Pekau and V. Batta, 'Seismic crack propagation analysis of concrete structures using boundary elements', *Int. j. numer. methods eng.* **35**, 1547–1564 (1992).
11. S. Mindess, 'Fracture toughness testing of cement and concrete', in A. Carpinteri and A. R. Ingraffea (eds), *Fracture Mechanics of Concrete: Material Characterization and Testing*, 1984, pp. 67–110.
12. E. Bruhwiler and F. H. Wittmann, 'Failure of dam concrete subjected to seismic loading conditions', *Eng. fract. mech.* **35**, 565–571 (1989).
13. R. Tinawi and L. Guizani, 'Formulation of hydrodynamic pressures in cracks due to earthquakes in concrete dams'. *Earthquake eng. struct. dyn.* **23**, 699–715 (1994).
14. 'Design of gravity dams', Bureau of Reclamation, United States Department of the Interior, Denver, CO, 1976.
15. 'Engineering guidelines for the evaluation of hydropower projects', United States Federal Energy Regulatory Commission, Office of Hydro Power Licensing, Washington, DC, 1991.
16. S. S. Saini and J. Krishna, 'Overturning of top profile of the Koyna dam during severe ground motion', *Earthquake eng. struct. dyn.* **2**, 207–217 (1974).